Potential climate change effects on groundwater recharge in the High Plains Aquifer, USA

Russell S. Crosbie,[1] Bridget R. Scanlon,[2] Freddie S. Mpelasoka,[3] Robert C. Reedy,[2] John B. Gates,[4] and Lu Zhang[3]

Received 19 December 2012; revised 24 March 2013; accepted 3 May 2013.

[1] Considering that past climate changes have significantly impacted groundwater resources, quantitative predictions of climate change effects on groundwater recharge may be valuable for effective management of future water resources. This study used 16 global climate models (GCMs) and three global warming scenarios to investigate changes in groundwater recharge rates for a 2050 climate relative to a 1990 climate in the U.S. High Plains region. Groundwater recharge was modeled using the Soil-Vegetation-Atmosphere-Transfer model WAVES for a variety of soil and vegetation types representative of the High Plains. The median projection under a 2050 climate includes increased recharge in the Northern High Plains (+8%), a slight decrease in the Central High Plains (−3%), and a larger decrease in the Southern High Plains (−10%), amplifying the current spatial trend in recharge from north to south. There is considerable uncertainty in both the magnitude and direction of these changes in recharge projections. Predicted changes in recharge between dry and wet future climate scenarios encompass both an increase and decrease in recharge rates, with the magnitude of this range greater than 50% of current recharge. On a proportional basis, sensitivity of recharge to changes in rainfall indicates that areas with high current recharge rates are least sensitive to change in rainfall and vice versa. Sensitivity analyses indicate an amplification of change in recharge compared to change in rainfall, and this amplification is in the range of 1–6 with an average of 2.5–3.5 depending upon the global warming scenario.

Citation: Crosbie, R. S., B. R. Scanlon, F. S. Mpelasoka, R. C. Reedy, J. B. Gates, and L. Zhang (2013), Potential climate change effects on groundwater recharge in the High Plains Aquifer, USA, *Water Resour. Res.*, *49*, doi:10.1002/wrcr.20292.

1. Introduction

[2] The most recent Intergovernmental Panel on Climate Change (IPCC) report noted a comparative lack of studies addressing the effects of climate change on groundwater [*Intergovernmental Panel on Climate Change (IPCC)*, 2007]. This challenge has been taken up by the groundwater research community and has resulted in an increasing focus of study on this topic in recent years [*Green et al.*, 2011; *Taylor et al.*, 2013], although there still remains many aspects of the climate change effects on groundwater that have not been well studied. The most direct method in which climate change will impact groundwater resources is by modifying the renewable portion of groundwater storage through changes in recharge. Knowledge of future recharge rates is desirable in order to promote proactive management of groundwater, as historical observations may not be an appropriate basis for management under a future climate.

[3] The High Plains Aquifer is a very important source of water for the United States. The High Plains Aquifer is ranked first in terms of volume of groundwater extracted in the United States; for the year 2000, 16 km^3 was extracted, of which 97% was for irrigation [*Maupin and Barber*, 2005]. This irrigation water underpins a market value of agricultural products of $35 billion or more than 10% of the national total [*National Agricultural Statistics Services*, 2011]. However, groundwater extractions currently exceed recharge by up to a factor of 10 in some areas, resulting in depletion of storage mostly in the central and southern High Plains. Depletion has averaged 5.7 $km^3\ yr^{-1}$ since irrigation development began in the 1950s [*Scanlon et al.*, 2012], making the High Plains a globally significant hotspot of groundwater depletion [*Wada et al.*, 2010].

[4] Previous studies on climate change and recharge in the High Plains have mainly focused on paleoclimate and

Additional supporting information may be found in the online version of this article.

[1]CSIRO Water for a Healthy Country National Research Flagship, CSIRO Land and Water, Glen Osmond, South Australia, Australia.
[2]Bureau of Economic Geology, Jackson School of Geosciences, University of Texas at Austin, Austin, Texas, USA.
[3]CSIRO Water for a Healthy Country National Research Flagship, CSIRO Land and Water, Canberra, Australian Capital Territory, Australia.
[4]Department of Earth and Atmospheric Sciences, University of Nebraska–Lincoln, Lincoln, Nebraska, USA.

Corresponding author: R. S. Crosbie, CSIRO Water for a Healthy Country National Research Flagship, CSIRO Land and Water, PMB 2, Glen Osmond, SA 5064, Australia. (russell.crosbie@csiro.au)

0043-1397/13/10.1002/wrcr.20292

how current recharge (particularly in the Southern High Plains (SHP) and Central High Plains (CHP)) is much lower than it has been under past climatic conditions during the Pleistocene [*McMahon et al*., 2006; *Scanlon et al*., 2012]. There have only been two previous studies that have investigated recharge under a future climate for the High Plains. *Rosenberg et al*. [1999] used three global climate models (GCMs) and a variety of global warming and CO_2 concentration scenarios for two river basins in the Northern High Plains (NHP) and CHP to make projections of future recharge in the range of −80% to −1% relative to the historical baseline. *Ng et al*. [2010] investigated recharge under a 2090 climate relative to a 1990 climate using five GCMs at a point scale in the SHP, projecting changes in recharge of between −75% and +35%.

[5] Previous studies into the effect of climate change on groundwater recharge in the High Plains did not consider the entire aquifer, and did not have the spatial resolution necessary to compare results between southern, central, and northern subregions. They also did not consider differences between irrigated and dryland agricultural land uses. This study will address these knowledge gaps; specifically, the aims of this study are (1) to make projections of changes in diffuse recharge under a range of future climate variants for a 2050 climate relative to a 1990 climate for the entire High Plains, including quantification of uncertainty ranges in recharge projections; (2) to investigate whether the recharge sensitivity to climate change is different under irrigated and dryland agriculture; and (3) to make recommendations for water resource managers to enable effective planning for future water availability.

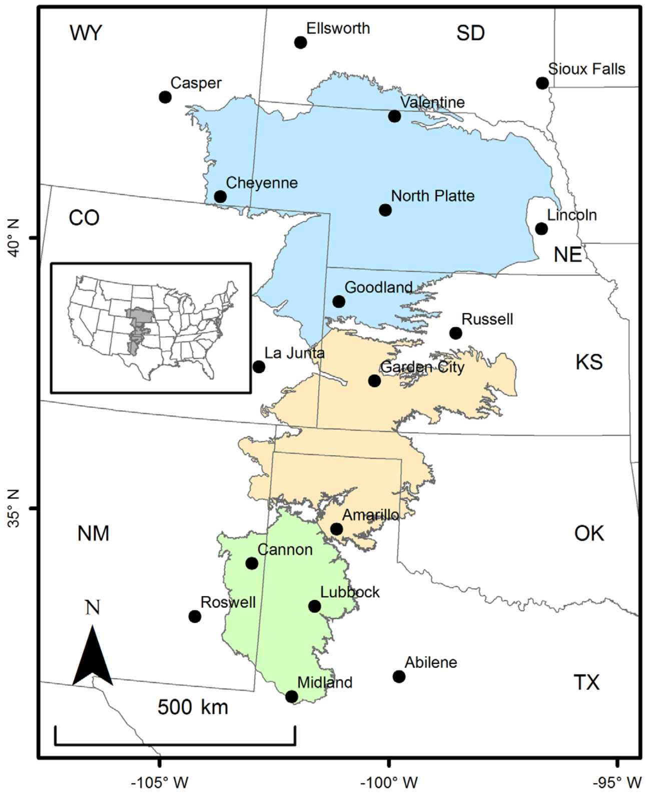

Figure 1. Location of the High Plains Aquifer within the US (inset) and the 17 climate stations used in the modeling. The Northern High Plains (NHP) is colored blue, the Central High Plains (CHP) beige, and the Southern High Plains (SHP) green.

2. Background to Study Area

[6] The High Plains Aquifer extends across an area of 450,000 km^2 in the central United States, covering parts of eight states (Figure 1). Mean annual rainfall (1982–2011) is 520 mm yr^{-1} across the region with a summer rainfall maximum and strong rainfall gradient from west to east. In contrast, the temperature gradient is north-south. Mean annual potential evapotranspiration (ET) exceeds mean annual rainfall throughout the region. The general climate change projections from the *IPCC* [2007] for this region at the end of this century are for an almost linear increase in temperature between 2 and 5°C and for a change in rainfall across the aquifer with an increase in the north and a decrease in the south.

[7] The aquifer system includes late Tertiary and Quaternary age sediments consisting of alluvial, dune-sand, and valley-fill deposits with a maximum thickness of about 200 m [*Weeks et al*., 1988]. The aquifer is unconfined across its extent, and the preagricultural development depth to water varied from less than 5 m along rivers (predominately in the NHP) up to 100 m for parts of the CHP and SHP [*Scanlon et al*., 2012].

[8] The native vegetation was primarily perennial prairie grassland with very few trees. Development of the area began with dryland agriculture in the late 1800s followed by rapid expansion of irrigated agriculture in the 1950s [*Colaizzi et al*., 2009]; irrigated land now covers ~12% of the region [*Qi et al*., 2002]. Water for irrigation is sourced from groundwater in the south and central regions and from a combination of groundwater (86%) and surface water (16%) in the north (2005 data, [*Kenny et al*., 2009]). If groundwater depletion is spread over the entire High Plains Aquifer, it would result in a mean water table decline of 4.2 m; however, there is almost no depletion in the north, and water table mounds are found near parts of the Platte River, whereas depletion is focused in the CHP and SHP with water table declines of as much as 70 m in Texas [*McGuire*, 2009]. The spatial variation in storage depletion is primarily controlled by differences in recharge from the NHP to the SHP, which in turn is strongly affected by variations in soil texture [*Scanlon et al*., 2012].

[9] The predevelopment recharge for the entire aquifer has recently been estimated using a chloride mass balance technique [*Scanlon et al*., 2012]. The NHP has the highest recharge of up to 210 mm yr^{-1} in coarse-textured soils within the Nebraska Sand Hills. Most of the CHP has a recharge rate of 5–25 mm yr^{-1} with some higher and lower areas associated with different soil textures. The SHP has an average recharge rate of 10 mm yr^{-1}, although this occurs predominantly through focused recharge in ephemeral lakes or playas rather than diffuse recharge through the soil matrix (this average recharge rate only applies to part of the SHP as some areas were excluded from the *Scanlon et al*. [2012] study due to upward flow of groundwater from deeper aquifers).

[10] Recharge focused through playas in the SHP has been reported as 77 mm yr^{-1} [*Wood and Sanford*, 1995] and 60–120 mm yr^{-1} [*Scanlon and Goldsmith*, 1997], and this occurs over the 1.4% of the area of the SHP covered by playas [*Ng et al*., 2010]. The remaining 98.6% of the SHP contributed negligible amounts of recharge under native vegetation (<0.1 mm yr^{-1} [*Scanlon and Goldsmith*, 1997]).

[11] Agricultural development has resulted in increased deep drainage rates (water flux below the root zone as opposed to recharge at the water table) across the High Plains and has recharged the aquifer in parts of the central and southern High Plains, as shown by rising groundwater levels by up to 23 m [*Luckey and Becker*, 1999; *Scanlon et al*., 2005]. Increases in recharge on some other areas may be masked by depletion related to groundwater-based irrigation. Because irrigation is sourced with groundwater, in other areas of the CHP and SHP, rates of water table declines generally exceed the increased drainage rates, and the net impact on groundwater storage is negative. In addition, fine-textured soils and/or deep water tables in many regions could result in lag times of decades to centuries for increased deep drainage to reach the water table and to translate to increased recharge [*McMahon et al*., 2006; *Scanlon et al*., 2010b]. It is generally assumed that deep drainage will become recharged, but this is only the case if there is no interflow discharge or perching before the deep drainage reaches the water table. Under irrigated agriculture in the CHP reported deep drainage rates range from 21 to 54 mm yr^{-1} for Texas [*Scanlon et al*., 2010b] and western Kansas [*McMahon et al*., 2003] and up to 165 mm yr^{-1} in eastern Kansas, where rainfall is higher and soil texture is coarser [*Sophocleous*, 2004]. In the SHP, reported deep drainage under dryland agriculture ranges from 4.8 to 92 mm yr^{-1} with a median of 21 mm yr^{-1} [*Scanlon et al*., 2007] and from 18 to 97 mm yr^{-1} with a median of 41 mm yr^{-1} under irrigated agriculture [*Scanlon et al*., 2010a], this is an increase over native vegetation, which has negligible diffuse recharge [*Scanlon et al*., 2007]. A water balance approach was used to estimate recharge and discharge in the Nebraska Sand Hills based on gridded rainfall and ET data [*Szilagyi et al*., 2011], and this study found an average recharge rate of 72 mm yr^{-1}, which corresponded well with chloride-based estimates.

[12] The objectives of water resources management vary across the different regions of the aquifer. In Nebraska (NHP), the focus is on maintaining baseflow in streams in order to fulfill interstate agreements and protect aquatic habitat for migratory birds [*Luckey et al*., 2007]. In Texas (CHP and SHP), there is little or no connection between surface water and groundwater, and the water resource is treated as a fossil reserve where there is a planned depletion of storage [*Scanlon et al*., 2012]. Kansas (CHP) has a mixture of these two extremes, with the west having planned depletion and in the east the priority is stabilizing groundwater levels to maintain stream baseflow [*Sophocleous*, 2012].

3. Methods

[13] The methods used in this study were selected to mirror those used by *Crosbie et al*. [2013] for investigating climate change impacts on recharge in Australia. This approach was selected in order to allow for comparisons between the current study and the previous study without added uncertainty stemming from methodological differences (comprehensive comparison between results from the High Plains and Australia will be the subject of a future investigation). The method consists of three main steps: (1) point-scale modeling of recharge under historical and future climates using a numerical model; (2) upscaling the point results to the entire High Plains Aquifer; and (3) aggregating the results from the 48 future climate variants down to three so that the results can be communicated effectively.

3.1. Point-Scale Modeling

[14] Groundwater recharge was modeled using a slightly modified version [*McCallum et al*., 2010] of the WAVES model [*Zhang and Dawes*, 1998]. WAVES is a soil-vegetation-atmosphere-transfer model that achieves a balance in its modeling complexity between carbon, energy, and water balances [*Zhang and Dawes*, 1998]. Its ability to simulate plant physiology allows changes in temperature and CO_2 to impact transpiration, and therefore recharge. It uses the Penman-Monteith equation [*Monteith*, 1965] for simulation of the energy balance, and this allows ET to be affected by dynamic vegetation growth responding to availability of water, nutrients, and light [*Wu et al*., 1994]. WAVES uses Richards' equation for modeling unsaturated flow, which has the advantage of allowing water movement to be simulated under relatively dry conditions [*Scanlon et al*., 2002]. WAVES has been shown to be able to reproduce measured field data in a variety of environments [*Zhang et al*., 1996, 1999; *Wang et al*., 2001; *Crosbie et al*., 2008] and has previously been used in modeling recharge under future climate scenarios [*Green et al*., 2007; *Crosbie et al*., 2010b, 2013]. WAVES has also been shown to perform similar to three other hydrological models with different conceptualizations (WAVES-C, HELP, and SIMHYD) in a comparison study of the climate change impacts on recharge [*Crosbie et al*., 2011].

[15] WAVES requires three main data sets: climate, soils, and vegetation. The upper boundary condition is forced with climate data and the lower boundary condition is free drainage, consistent with previous studies of the impact of climate change on recharge [*Green et al*., 2007; *Crosbie et al*., 2010b, 2013]. Drainage below the base of a 4 m soil column is assumed to become groundwater recharge; this is considered potential diffuse recharge. It is assumed that the water table is deeper than 4 m and does not affect the assumption of the free draining lower boundary condition. Localized recharge and the time lag between deep drainage (below the root zone) and recharge (at the water table) [*Cook et al*., 2002] is not considered in the present analysis. Under predevelopment conditions, there is no doubt that localized recharge was dominant in the SHP [*Gurdak and Roe*, 2010]. However, under the current land use, this is not the case. The field estimates of deep drainage beneath different land uses allow us to calculate an approximate areal recharge rate for predevelopment and postdevelopment cases for the SHP (Table 1). This simple analysis shows that focused recharge beneath playas was 92% of areal recharge under the predevelopment case but

Table 1. Calculated Areal Recharge Rates for Predevelopment and Postdevelopment Cases for the SHP Using the Median Recharge Rates Reported From Field Studies Under Different Land Uses

	Recharge (mm yr^{-1})	Area (%)		Areal Recharge (mm yr^{-1})	
		Pre	Post	Pre	Post
Playas	77	1.4	1.4	1.1	1.1
Perennial veg	0.1	98.6	52.2	0.1	0.05
Dryland Agriculture	21	0	34.8	0	7.3
Irrigated Agriculture	41	0	11.6	0	4.8
Total				1.2	13.2

only 8% of areal recharge under the postdevelopment case. As we did not have a predevelopment scenario in the modeling for this paper, the assumption of diffuse recharge is valid, even for the SHP.

[16] Point-scale modeling was conducted at 17 sites across the High Plains (Table 2 and Figure 1) selected to cover the rainfall gradient (Figure 2). The historical climate (30 year period from 1982 to 2011) was used as a baseline and assumed to be representative of a 1990 climate. For each of the 17 points, daily rainfall and minimum, maximum, and dew point temperatures were obtained from the National Climate Data Center (http://www.ncdc.noaa.gov/). (All precipitation was input into WAVES as rainfall, and snowmelt processes were not considered). The temperature data were then used to calculate the vapor pressure deficit (VPD) as used by WAVES. The other climate variable needed by WAVES is solar radiation, which was obtained from National Centre for Atmospheric Research/National Centre for Environmental Prediction (NCAR/NCEP) reanalysis data [*Kalnay et al.*, 1996]. The 30 year climate time series was repeated in the model input files to create a 60 year time series. The first 30 years of the simulation were discarded as a model spin-up period, and the results were reported for the second 30 year period. Atmospheric CO_2 concentration for the historical baseline period was assumed to be a constant 353 ppm, as observed in 1990 [*IPCC*, 2007]. A constant was used rather than a time series, as the modeling undertaken here is investigating a projected 2050 climate relative to a 1990 climate rather than a transient projection. Similarly, the simulated recharge represents recharge under a 2050 climate relative to recharge modeled under a 1990 climate, as opposed to recharge modeled in 2050 relative to 1990. The distinction here is that a transient projection is not being made and therefore the time lags associated with the change in recharge are not considered.

Table 2. Mean Annual Rainfall (P) and Potential Evapotranspiration (PET) [*Allen et al.*, 1998] for the 30 Year Period 1982–2011 for Each of the 17 Climate Stations Shown in Figure 1 in Order of Ascending Rainfall

Climate Station	State	P (mm yr^{-1})	PET (mm yr^{-1})	P/PET
La Junta	CO	296	1330	0.22
Roswell	NM	310	1346	0.23
Casper	WY	344	1229	0.28
Midland	TX	387	1423	0.27
Cheyenne	WY	393	1289	0.30
Valentine	NE	450	1214	0.37
Cannon	NM	470	1343	0.35
Ellsworth	SD	475	1159	0.41
Garden City	KS	488	1324	0.37
Lubbock	TX	494	1343	0.37
Goodland	KS	525	1292	0.41
North Platte	NE	526	1264	0.42
Amarillo	TX	539	1344	0.40
Russell	KS	615	1322	0.47
Abilene	TX	632	1397	0.45
Sioux Falls	SD	718	1246	0.58
Lincoln	NE	733	1299	0.56

[17] The future climate global warming scenarios were inferred from the *IPCC* [2007] to represent the range of Special Report on Emission Scenarios (SRES) scenarios [*Nakicenovic and Swart*, 2000]. Three scenarios for a 2050 climate relative to a 1990 climate were used:

[18] (1) Low global warming: +1.0°C, 478 ppm CO_2;

[19] (2) Medium global warming: +1.7°C, 523 ppm CO_2; and

[20] (3) High global warming: +2.4°C, 567 ppm CO_2.

[21] The use of three global warming scenarios combined with 16 GCMs was an attempt to incorporate as much uncertainty in climate projections as possible into the recharge projections [*Crosbie et al.*, 2011; *Holman et al.*, 2012]. These 16 GCMs were selected because they had daily data archived by the World Climate Research Programme's Coupled Model Intercomparison Project phase 3 (CMIP3) multimodel data set [*Meehl et al.*, 2007] and are the same 16 GCMs as used by *Crosbie et al.* [2013]. The CMIP3 model data were used rather than the CMIP5 model data to enable a comparison to previous work.

[22] A time series of climate variables for the future climate scenarios was derived from the 16 GCMs (Table 3) using the daily scaling method of *Chiew et al.* [2009]. The daily scaling approach is relatively simple and was used because it produced results in between the range of two more sophisticated approaches [*Crosbie et al.*, 2011]. The reader is referred to *Chiew et al.* [2009] for full details of the daily scaling methodology as only a brief summary is presented here. Archived monthly simulations from the 16 GCMs were analyzed to estimate the change in rainfall, temperature, humidity, and solar radiation per degree of global warming on a seasonal basis. The percent changes in the climate variables per degree of global warming for each of the four seasons from the 16 GCMs were then multiplied by the three levels of global warming to obtain 48 sets of "seasonal scaling" factors. These seasonal scaling factors were then used to scale the historical daily climate data from 1982 to 2011 to obtain 48 future climate variants, each with 30 years of daily climate data. The future VPD was calculated from the future humidity and temperature data. The temporal sequencing of rainfall remains from the historical time series, but changes in the daily rainfall intensity were then taken into account by scaling different rainfall amounts differently (i.e., generally increased rainfall intensity for the 2050 climate compared to the 1990 climate).

[23] The soil data required by WAVES are the soil moisture and hydraulic conductivity characteristic curves using the functions of *Broadbridge and White* [1998]. These data were inferred from information from the State Soil Geographic (STATSGO) Data Base [*Natural Resources Conservation Service (NRCS)*, 2006]. The percentage clay

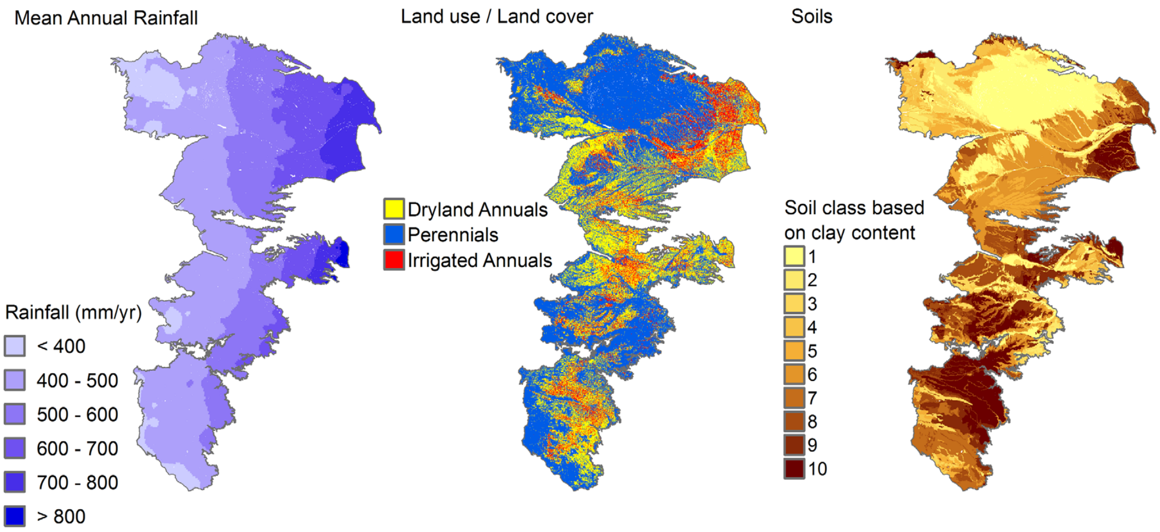

Figure 2. Spatial inputs used in the upscaling showing mean annual rainfall for the period 1982–2011, the reclassified land cover map, and the classification of soil types.

content data layer was used to classify the High Plains into 10 soil classes (Figure 2 and Table 4), and the soil textural and hydraulic conductivity variables were used to create the WAVES input files. The STATSGO soil profiles were simplified to be homogeneous and isotropic within each of the 10 classes. Considering that the average percentage of clay content of a soil profile has been shown to be a good correlate for recharge [*Wohling et al*., 2012], the profile homogenization is a reasonable simplification.

[24] The land use/land cover (LU/LC) types modeled for this study are dryland (or rainfed) cropland, irrigated cropland, and perennial grasses. Model parameters for all LU/LC types were obtained from the WAVES User Manual, which in turn are based on diverse information sources on plant physiology [*Dawes et al*., 2004]. The same parameters were used for both dryland and irrigated crops, representative of an annual C4 crop; the difference between them is the addition of 300 mm yr^{-1} of irrigation water applied in equal increments each week throughout the growing season. The amount and distribution of applied irrigation water is the same for the historical and future climate scenarios as we are not simulating irrigation scheduling or improved water management through new technologies. Under a future climate, irrigation amounts applied could be higher due to atmospheric demand or could be lower due to efficiencies of CO_2 fertilization and improved irrigation technologies. The applied irrigation is considered as a hypothetical scenario so that the effect of climate change upon recharge can be investigated without the added complexities of irrigation management; however, the applied water is within the range of published annual irrigation amounts throughout the High Plains [*McMahon et al*., 2006].

[25] Only a narrow range of LU/LC types were used here because field estimates of recharge do not support the use

Table 3. List of the 16 GCMs Used in This Study and the Abbreviations Used in the Figures in Supporting Information[a]

Organization	Country	CMIP3 I.D.	Abbrev.
Bjerknes Centre for Climate Research	Norway	BCCR-BCM2.0	BCCR
Canadian Centre for Climate Modelling & Analysis	Canada	CGCM3.1(T63)	CCCMA
Météo-France/Centre National de Recherches Météorologiques	France	CNRM-CM3	CNRM
CSIRO Atmospheric Research	Australia	CSIRO-Mk3.0	CSIRO MK3.0
CSIRO Atmospheric Research	Australia	CSIRO-Mk3.5	CSIRO MK3.5
Max Planck Institute for Meteorology	Germany	ECHAM5/MPI-OM	MPI
Meteorological Institute of the University of Bonn, Meteorological Research Institute of KMA, and Model and Data group.	Germany/Korea	ECHO-G	MIUB
US Dept. of Commerce/NOAA/Geophysical Fluid Dynamics Laboratory	USA	GFDL-CM2.0	GFDL CM2.0
US Dept. of Commerce/NOAA/Geophysical Fluid Dynamics Laboratory	USA	GFDL-CM2.1	GFDL CM2.1
NASA/Goddard Institute for Space Studies	USA	GISS-ER	GISS
Instituto Nazionale di Geofisica e Vulcanologia	Italy	INGV-SXG	INGV
Institute for Numerical Mathematics	Russia	INM-CM3.0	INMCM
Institut Pierre Simon Laplace	France	IPSL-CM4	IPSL
Center for Climate System Research (The University of Tokyo), National Institute for Environmental Studies, and Frontier Research Center for Global Change (JAMSTEC)	Japan	MIROC3.2(medres)	MIROC
Meteorological Research Institute	Japan	MRI-CGCM2.3.2	MRI
National Center for Atmospheric Research	USA	PCM	NCAR

[a]The list is alphabetical by CMIP3 ID.

Table 4. Soils Information Extracted From the STATSGO Database [*NRCS*, 2006][a]

Class	k (m d^{-1})	AWC (%)	Sand (%)	Silt (%)	Clay (%)	Texture
1	1.054	7.7	90.1	4.8	5.1	Sand
2	0.493	11.3	69.2	19.0	11.8	Sandy loam
3	0.400	12.6	61.5	24.8	13.7	Sandy loam
4	0.280	12.1	55.6	27.1	17.3	Sandy loam
5	0.164	15.7	33.7	46.3	20.0	Loam
6	0.140	18.0	20.4	57.5	22.1	Silt loam
7	0.149	15.4	35.7	40.0	24.3	Loam
8	0.114	16.7	27.6	46.0	26.4	Loam
9	0.104	15.9	30.4	40.3	29.3	Clay loam
10	0.054	15.8	26.1	36.3	37.6	Clay loam

[a]Classes are as shown in Figure 2. (k is saturated hydraulic conductivity of the soil, and AWC is plant available water capacity.)

of many classes [*Petheram et al.*, 2002; *Scanlon et al.*, 2006; *Crosbie et al.*, 2010a; *Kim and Jackson*, 2012]. The extremes of LU/LC types for recharge would be bare soil and forests, neither of which occupy a significant proportion of the High Plains (0.1% and 0.8%, respectively [*Homer et al.*, 2007]). Although both C3 (e.g., wheat) and C4 (e.g., corn, cotton) crops are sown in the High Plains, we do not have enough information on the differences in recharge between them to justify more classes of LU/LC (see supporting information Figures S1 and S2).

[26] WAVES was used to model recharge for every combination of the 17 climate stations, 10 soil classes, three LU/LC types, and 49 climate scenarios for a total of 24,990 model runs.

3.2. Upscaling

[27] The point-scale modeling in WAVES was used to create a relationship between mean annual rainfall and mean annual recharge for every combination of climate, soil, and vegetation using the results from the 17 climate stations. The form of the relationship was a power function that was fitted using a least squares routine.

$$R_s = aP_s{}^b \tag{1}$$

where R_s is mean annual recharge (R) under a given scenario (s), P_s is mean annual rainfall (P) under a given scenario, and a and b are fitting parameters.

[28] This set of regression equations was used to upscale the point recharge estimates to an aquifer recharge raster at a grid resolution of 1 km using a raster of mean annual rainfall, soil type, and vegetation type as covariates (Figure 2). The historical baseline rainfall raster was obtained from PRISM (PRISM Climate Group, Oregon State University, http://prism.oregonstate.edu/), the soils raster was derived from the STATSGO map [*NRCS*, 2006], and the vegetation raster was reclassified from National Land Cover Data (NLCD 2001) [*Homer et al.*, 2007] with irrigated land coverage from *Qi et al.* [2002] spliced in. These disparate data sets have been rescaled to a common grid size of 1 km from 1:250,000 for the soils, 4 km for rainfall, and 30 m for vegetation and irrigation. Limitations on the appropriate scale of use of the results is based on the coarsest data set (soils), which should not be used below a county scale [*NRCS*, 2006]. The finest scale reported in this paper is at a state scale.

[29] The process of upscaling produced one historical baseline aquifer scale recharge raster and 48 recharge rasters for the future climate variants. Results are presented as future climate scenario recharge (R_s) relative to the historical climate recharge (R_h) as a recharge scaling factor for a given scenario (RSF$_s$) [*Crosbie et al.*, 2010b]:

$$\mathrm{RSF}_s = \frac{R_s}{R_h} \tag{2}$$

3.3. Aggregation

[30] The 48 future climate variant RSF rasters represent the uncertainty in the projection of the change in recharge for a 2050 climate relative to a 1990 climate due to different magnitudes of global warming in 2050 and differences among GCMs (although there are other sources of uncertainty, such as downscaling, that are not addressed here). These 48 variants were fitted to a Pearson Type III distribution by global warming scenario at the grid cell scale, and the method for fitting the probability distribution is detailed in *Crosbie et al.* [2010b] and is not reproduced here. The Pearson Type III distribution was chosen as it has the ability to fit a distribution to skewed data, and *Crosbie et al.* [2010b] demonstrated that this distribution can adequately fit the RSF data used here. The distribution requires three parameters (mean, standard deviation, and skewness) to be calculated from the 16 RSF rasters at a grid cell scale (1 km).

[31] The 10, 50, and 90% exceedances from the probability distribution fitted to the data from each of the three global warming scenarios were selected for reporting the results to be consistent with previous work [*Crosbie et al.*, 2010b, 2013]. These nine points extracted from the three probability distributions have been further summarized down to just three future climate scenarios: a dry future climate is defined, for each grid cell, as the minimum of the 90% exceedance of RSF from the three global warming scenarios; the median future climate is defined as the median of the 50% exceedance from the three global warming scenarios; and the wet future climate is defined as the maximum of the 10% exceedance of RSF from the three global warming scenarios. These three summary scenarios represent the middle projection from the probability distributions (median future climate) and two projections from opposite tails of the distributions (wet and dry future climates).

3.4. Recharge Sensitivity to Climate Change

[32] The relationship between the change in mean annual recharge and the change in mean annual rainfall was evaluated in order to investigate sensitivity of recharge to climate change for the different vegetation types. The slope of this relationship represents the sensitivity of recharge to a change in rainfall, and the intercept of this relationship shows the sensitivity of recharge to all the other variables excluding the change in mean annual rainfall (e.g., changes in rainfall intensity, temperatures, CO_2 fertilization, etc. [*Crosbie et al.*, 2010b, 2012]).

[33] These relationships can be investigated at the point scale using the WAVES simulations and can also be investigated at the scale of the entire aquifer using the recharge raster maps. At the point scale the change in rainfall and recharge is plotted for a particular combination of climate station, soil type, and vegetation type for each global warming scenario using the 16 GCMs, and a linear

regression line is fitted to the data points to calculate the slope and intercept. At the scale of the entire aquifer the relationships are developed at a grid cell scale in the same way as the point scale using rasters from each of the 16 GCMs for each global warming scenario.

3.5. Uncertainty

[34] Each step in the modeling chain has considerable uncertainty, and these uncertainties propagate through to the final results. The point-scale modeling of historical recharge has a similar uncertainty to the field recharge estimates [*Crosbie et al.*, 2010a, 2010b], which can be mitigated by constraining the modeling results with field-based estimates. As the future climate results are reported relative to the historical baseline climate, uncertainty due to the unknown recharge under the historical climate is minimized, provided the historical climate results are consistent with field observations. Similarly, the upscaling method used will not introduce significant additional uncertainty, provided the regression fits are similar between the historical and future climates as the results are reported as recharge under future climate relative to historical climate. The major source of uncertainty in the future projections of recharge is from the GCMs projections of the future climate [*Crosbie et al.*, 2011], which can be taken into account by using as many different GCMs as possible. Downscaling of the future climate from the GCMs is also a source of uncertainty in the recharge projections [*Holman et al.*, 2009; *Mileham et al.*, 2009] but less than the uncertainty due to the GCMs themselves [*Crosbie et al.*, 2011]. The selected downscaling method preserves the average changes from the GCMs while performing within the range of more sophisticated methods [*Crosbie et al.*, 2011]. The final results are presented as a wet, median, and dry future recharge, which uses uncertainty in the projections to present a simplified range of results that are readily understood.

4. Results

4.1. Baseline Historical Recharge

[35] Recharge from the historical climate simulations in WAVES was summed for the 30 year period 1982–2011 and used to produce relationships between mean annual rainfall and mean annual recharge for every combination of soil and vegetation (e.g., Figure 3). In all cases, these relationships are statistically significant ($p < 0.05$) with a mean r^2 of 0.79 (the complete list of regression equations is provided in supporting information Table S1). The trends show expected relationships between recharge and rainfall (positive correlation), soil texture (higher rates under coarser-textured soils), and vegetation (lower recharge rates under perennial vegetation). These relationships were used to create the historical recharge raster that was used as a baseline to compare the future climate recharge.

[36] The historical climate baseline raster (Figure 4) produces spatial trends that are consistent with previously published recharge estimates for the High Plains. In areas of perennial vegetation, it is most appropriate to compare the current recharge map with that produced by *Scanlon et al.* [2012] for a predevelopment case, and in both maps the highest recharge is in the NHP associated with coarse-textured soils, the lowest recharge in both cases is in the CHP and SHP associated with fine-textured soils (the current map is lower in the SHP than the areas covered by the *Scanlon et al.* [2012] recharge map for perennial vegetation because only diffuse recharge is simulated and focused recharge beneath playas is omitted). For the NHP, the recharge map of *Szilagyi et al.* [2011] is not directly comparable to the map produced in this study due to different definitions of recharge, but in both cases there is a very strong west to east recharge gradient associated with the rainfall gradient. The recharge under annual and irrigated vegetation in the CHP and SHP is much greater than under perennial vegetation consistent with field measurements [*McMahon et al.*, 2003; *Scanlon et al.*, 2010a, 2010b] and highest recharge in the High Plains is in eastern Nebraska and eastern Kansas associated with irrigation on coarse-textured soils.

4.2. Future Recharge Projections

[37] Projections of changes in rainfall among the various GCMs differ (supporting information Figures S4–S6) but do show a general trend with more than half of the GCMs projecting an increase in rainfall for the NHP, and very few GCMs projecting an increase in rainfall for the SHP (Figure 5). The trend with increasing global warming is for

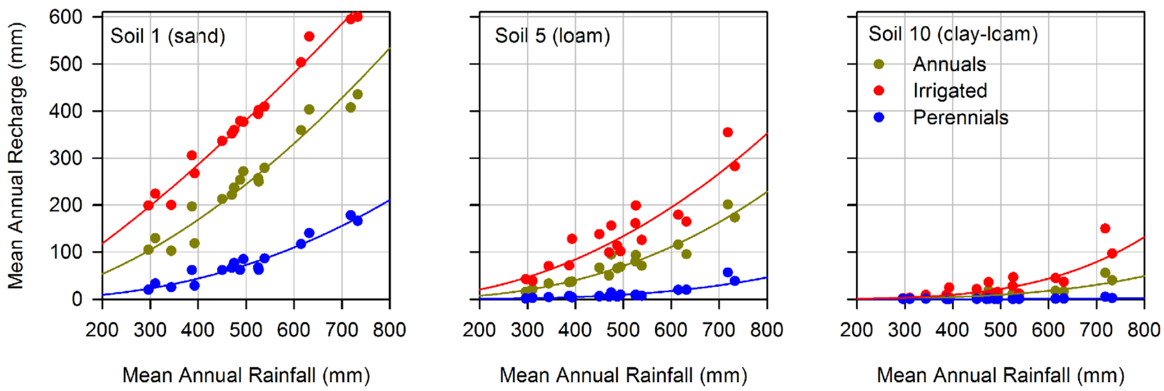

Figure 3. Mean annual recharge simulated using WAVES for the historical baseline scenario (1982–2011) for three soil classes (the other seven soil classes are shown in supporting information Figure S3) and three LU/LC types at each of the 17 climate stations. Also shown are curves fitted through the 17 data points used for upscaling point-scale recharge.

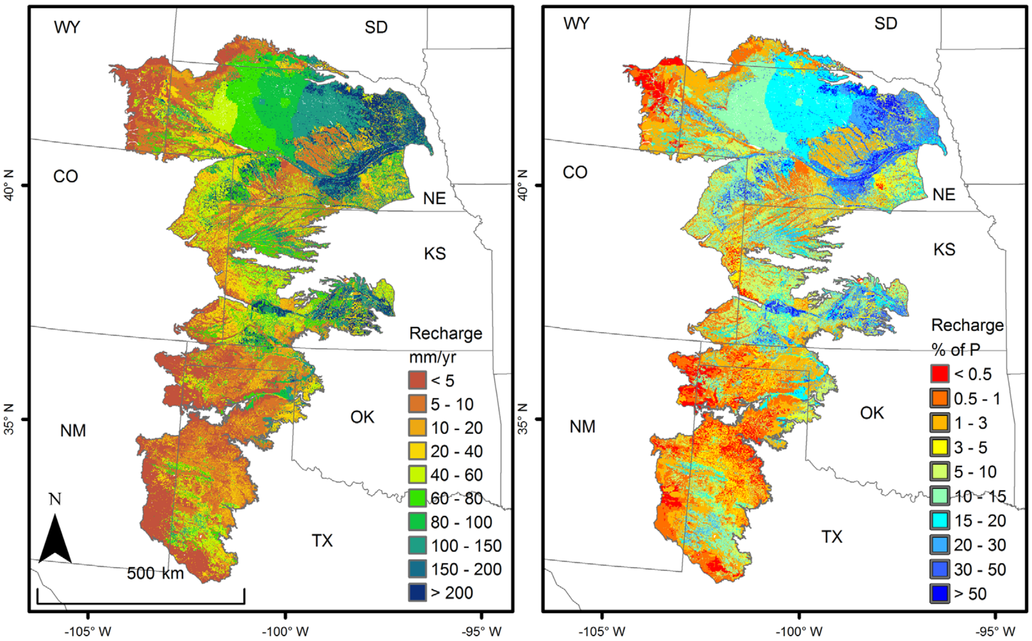

Figure 4. Simulated historical recharge for the period 1982–2011 used as a baseline for the future climate scenarios. (left) Recharge in mm yr^{-1} and (right) Recharge as a percentage of rainfall.

rainfall projections to diverge from the historical rainfall; the range between the highest and lowest projections increases with increasing global warming. For the NHP the median (range) of the 16 GCMs is for 1% (−7% to +5%), 2% (−11% to +9%), and 3% (−16% to +12%) increase in rainfall for the low, medium, and high global warming scenarios, respectively. For the CHP, the median (range) projections for the same scenarios are for a 2% (−9% to +3%), 4% (−15% to +5%), and 5% (−21% to +7%) reduction in rainfall, and for the SHP, a 5% (−10% to +3%), 8% (−15% to +5%), and 11% (−24% to +7%) reduction in rainfall.

[38] The future climate WAVES simulations were treated similarly to the historical climate model runs in developing relationships between average annual rainfall and recharge, and in all cases, the relationships are statistically significant ($p < 0.05$; mean r^2 of 0.79, the full list of regression equations is given in supporting information Table S1).

[39] The trend for future recharge projections differs from the trend of the future rainfall projections. For the low global warming scenario, more than half of the GCMs project an increase in recharge and with increasing global warming progressively fewer GCMs project an increase in

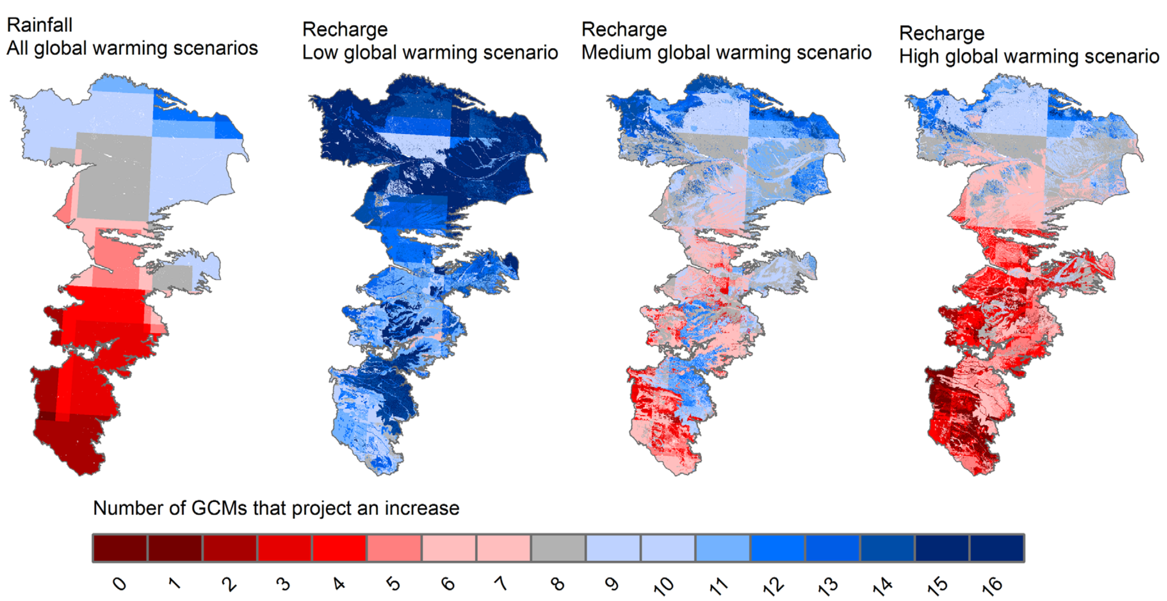

Figure 5. The number of GCMs that project an increase in rainfall or recharge for each global warming scenario.

recharge (Figure 5). For the high global warming scenario, only the northernmost part of the aquifer has more than half of the GCMs projecting an increase in recharge. The same trends can be seen when evaluating the individual GCMs (supporting information Figures S7–S9).

[40] After the individual RSF rasters for each GCM and global warming scenario were fitted to the probability distributions, some very clear trends between RSF values and global warming scenarios emerged (Figure 6). For the 90% exceedance for the low global warming scenario, the RSF projections for the majority of the aquifer are not statistically significant; however, with increasing global warming the 90% exceedances become statistically significant for most of the aquifer. For the medium and high global warming scenarios, RSF progressively decreases in magnitude compared to the low global warming scenario, indicating decreasing recharge. For the 50% exceedance of the low global warming scenario, recharge is projected to increase throughout most of the aquifer. For the medium global warming scenario, most of the aquifer does not have a statistically significant change in recharge, except for the very northern part of the aquifer with an increase in projected recharge and some parts of the south with a decrease in projected recharge. For the high global warming scenario and 50% exceedance, the majority of the north of the aquifer does not have a significant change in projected recharge, and most of the CHP and SHP have a statistically significant reduction in projected recharge. For the 10% exceedance for the low and medium global warming scenarios, all the aquifer has a projected increase in recharge, and the high global warming scenario continues this trend but with an increase in the area that does not have a statistically significant change in projected recharge. Overall, the trends shown here are for a greater reduction in recharge with increasing global warming for the 90% exceedances, an increase in recharge for the 50% exceedance for the low global warming scenario and then a progressive reduction in recharge with increasing global warming, and for the 10% exceedance increases in recharge are projected with only small changes in the magnitude of the change in recharge with increasing global warming.

[41] The results from fitting the RSF rasters to the probability distributions have simplified down to just three scenarios: dry, median, and wet (Figure 6). For the dry scenario, recharge is projected to decrease over the entire aquifer with a trend toward progressively greater reductions from north to south. For the median scenario, recharge is projected to increase in the NHP and decrease over most of the CHP and SHP. For the wet scenario, recharge is projected to increase over the entire aquifer.

[42] At a regional scale, the NHP has a median RSF projection of 1.08, ranging from 0.76 for the dry scenario to

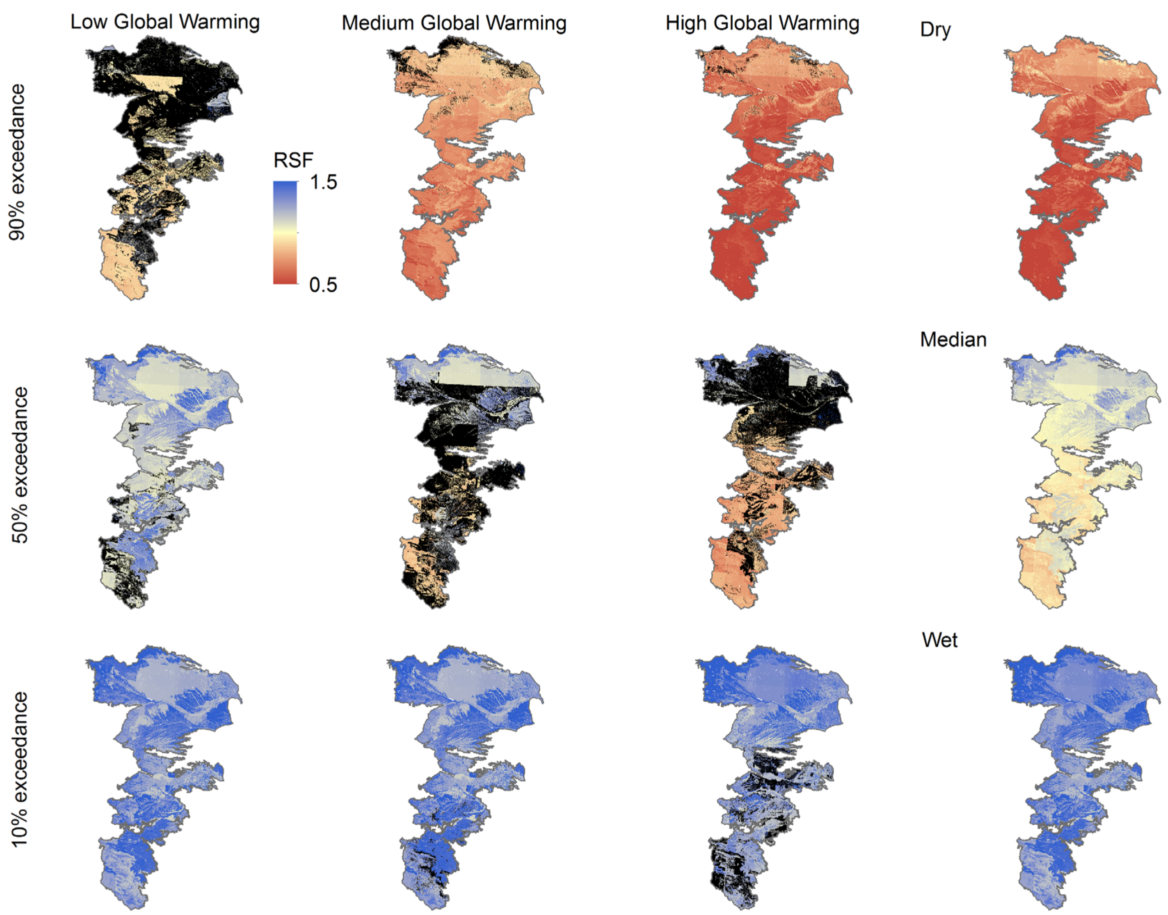

Figure 6. Results of fitting the RSF rasters to a Pearson type III probability distribution showing the 10, 50, and 90% exceedances for the three global warming scenarios and the aggregated wet, median, and dry projections for RSF. Black areas represent statistically insignificant changes in recharge.

Table 5. Baseline Recharge (*R*) for the Historical Climate Scenario for the 30 Year Period 1982–2011 and RSFs for Dry, Median, and Wet Future Climate Scenarios for the NHP, CHP, and SHP Regions and Eight States of the High Plains

Region/State	Area (km^2)	Baseline *R* (mm yr^{-1})	Dry RSF	Median RSF	Wet RSF
NHP	250,789	78	0.76	1.08	1.32
CHP	125,754	49	0.63	0.97	1.23
SHP	74,989	18	0.50	0.90	1.25
South Dakota	12,704	44	0.82	1.14	1.41
Wyoming	21,926	16	0.84	1.15	1.44
Nebraska	165,703	99	0.77	1.09	1.32
Colorado	34,457	39	0.69	1.02	1.27
Kansas	79,982	71	0.63	0.99	1.23
Oklahoma	19,812	34	0.59	0.96	1.23
Texas	92,525	21	0.52	0.91	1.24
New Mexico	24,459	9	0.50	0.88	1.24

1.32 for the wet scenario (Table 5). The CHP has a median RSF projection of 0.97, ranging from 0.63 for the dry scenario to 1.23 for the wet scenario. The SHP has a median RSF projection of 0.90 ranging from 0.50 for the dry scenario to 1.25 for the wet scenario. At a state scale, the results are similar with all states having a range in RSF projections that encompass both increases and decreases in recharge and for the median scenario a general progression from the greatest increases in recharge in the north and the greatest decreases in recharge in the south. For the median scenario, recharge is projected to increase in four states (SD 1.14, WY 1.15, NE 1.09, and CO 1.02) and decrease in the other four states (KS 0.99, OK 0.96, TX 0.91, and NM 0.88).

4.3. Recharge Sensitivity to Climate Change

[43] The sensitivity of recharge to climate change was evaluated by investigating the relationship between the change in rainfall and the change in recharge. To do this, three sites were selected to cover the range of climate and soils in the High Plains: Valentine, NE, on soil 1 (sand); Cheyenne, WY, on soil 5 (loam); and, Amarillo, TX, on soil 10 (clay-loam). The baseline recharge at these sites follows the trend with soils and vegetation, with the highest recharge in coarse-textured Valentine sandy soils: 336 mm yr^{-1} in irrigated annuals, 212 mm yr^{-1} in dryland annuals, and 61 mm yr^{-1} in perennials, followed by Cheyenne loamy soil with 128, 37, and 4 mm yr^{-1} and Amarillo with clay-loam soils with the lowest baseline recharge with 11, 8, and 0.2 mm yr^{-1}.

[44] There is a general trend across all three sites for the slope of the mean annual rainfall versus mean annual recharge to decrease with increasing recharge (Figure 7). The trend in the slopes is most evident at the Valentine site; the irrigated vegetation case has a slope of 1.18, the annuals 1.46, and the perennials 2.56 for the high global warming scenario. This represents the sensitivity of recharge to a change in rainfall, a slope of 2 means that for every increment of 1% change in rainfall there is a 2% change in recharge.

[45] The differences in the intercept of the relationship is most evident at the Cheyenne site, the low global warming scenario has the highest intercept for each vegetation type, and the intercept decreases with increasing global warming. The intercept in this relationship is the total sensitivity of recharge to all other variables that are not represented by the change in mean annual rainfall; this includes changes in rainfall intensity and seasonality, vegetation water use efficiency through changes in temperature, and the CO_2 fertilization effect, and also changes in potential ET (PET) having an impact upon actual ET.

[46] There is nothing specifically different about the sensitivity of recharge to climate change for the three LU/LC classes investigated. For the irrigated annuals case (Figure 7), it can be seen that the Valentine site has the shallowest slope and the Amarillo site has the steepest slope. This is demonstrating the inverse relationship between the sensitivity of recharge to a change in rainfall and the historical baseline recharge (Valentine has the highest baseline recharge and Amarillo the lowest). Further evidence for this is seen as the slopes for all three LU/LC classes are greater at Cheyenne than Valentine.

[47] These relationships between the change in rainfall and recharge can also be evaluated on a spatial basis (Figure 8). The same trends are evident at the spatial scale, as were seen at the point scale. The slope is lowest in areas of high recharge, is highest in areas of low recharge, and decreases slightly with increasing global warming. The intercept clearly decreases with increasing global warming.

5. Discussion

5.1. Relationship Between Recharge and Global Warming

[48] Model results show a trend with projected increases in recharge for the low global warming scenario and then a reduction in recharge with further increases in global warming that is not related to changes in rainfall. This result seems counterintuitive and needs further exploration. Previous studies where an increase in recharge was projected from a decrease in rainfall have invoked a variety of possible causes, including increased rainfall intensity [*Crosbie et al.*, 2012], changes in wet/dry spell duration [*Green et al.*, 2007], changes in the time required for annual vegetation to complete their life cycle [*McCallum et al.*, 2010], and reductions in leaf area index as vegetation is extended outside of its optimum temperature range [*McCallum et al.*, 2010]. These mechanisms are not (wholly) responsible for the results seen here as the increase in recharge is dependent on the magnitude of the projected global warming and not forming a linear trend with increased global warming as seen in the previous studies.

[49] To investigate this further, changes in the climate inputs to WAVES were analyzed for each global warming

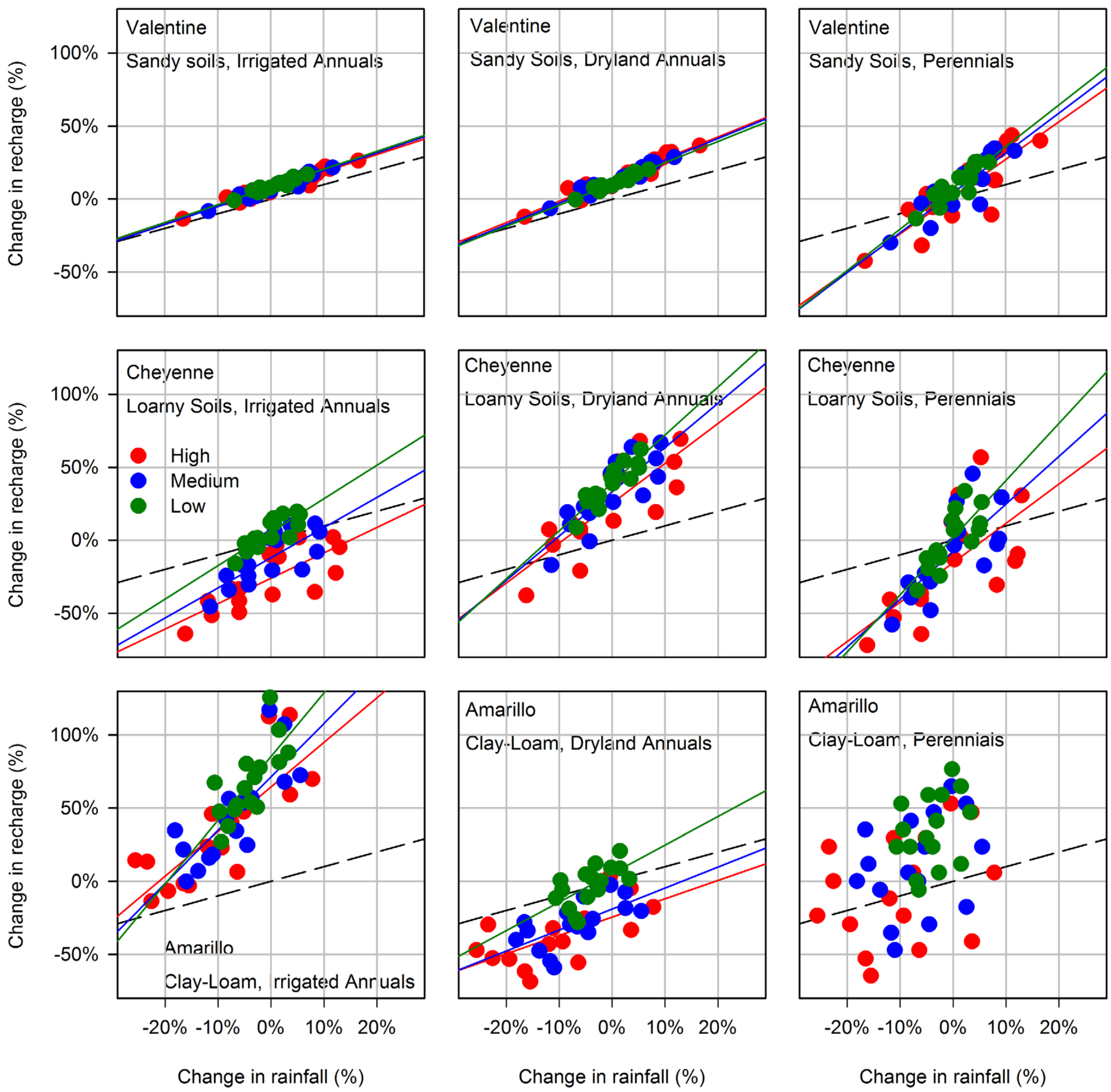

Figure 7. Relationship between a change in mean annual recharge relative to a change in mean annual rainfall for three locations with three different LU/LC for three global warming scenarios (low, medium, and high) using 16 GCMs. The black dashed line on each plot is a 1:1 line for reference.

scenario for the three climate stations used previously: Valentine, Cheyenne, and Amarillo (Figure 9). For the rainfall, Amarillo has a decreasing trend in the median of the 16 GCMs with increased global warming, Valentine has an increasing trend, and Cheyenne has no trend, and all three sites show greater variability among GCMs with increasing global warming. For both minimum and maximum temperatures, all three sites have the same trend with an increase in temperature with increasing global warming. Analysis of the VPD shows a decrease in VPD for the low global warming scenario, for all three sites, and an increase in the VPD with the medium and high global warming scenarios. This is attributed to a general increase in relative humidity (RH) across the 16 GCMs, for the low global warming scenario, the increased temperatures are not sufficient to offset the increased RH and so the VPD decreases, for the medium and high global warming scenarios, the increased temperatures result in an increase in VPD despite the increased RH. The solar radiation only changes slightly with increased global warming for all three sites.

[50] Since the WAVES model uses the Penman-Monteith equation [*Monteith*, 1965] for ET, we can use a variant of this model to investigate the changes in PET using the FAO56 reference ET (ET_0) [*Allen et al.*, 1998] as a common method across climate scenarios. The equation is:

$$ET_0 = \frac{0.408\Delta(R_n - G) + \gamma\frac{900}{T+273}u_2(e_s - e_a)}{\Delta + \gamma(1 + 0.34u_2)} \tag{3}$$

where R_n is net radiation, G is soil heat flux, T is mean daily temperature, u_2 is wind speed at 2 m height, e_s is saturation vapor pressure, e_a is actual vapor pressure, (VPD $= e_s - e_a$), Δ is slope of the vapor pressure curve, and γ is the psychrometric constant (the reader is referred to *Allen et al.* [1998] for a thorough description of this equation and its parameters).

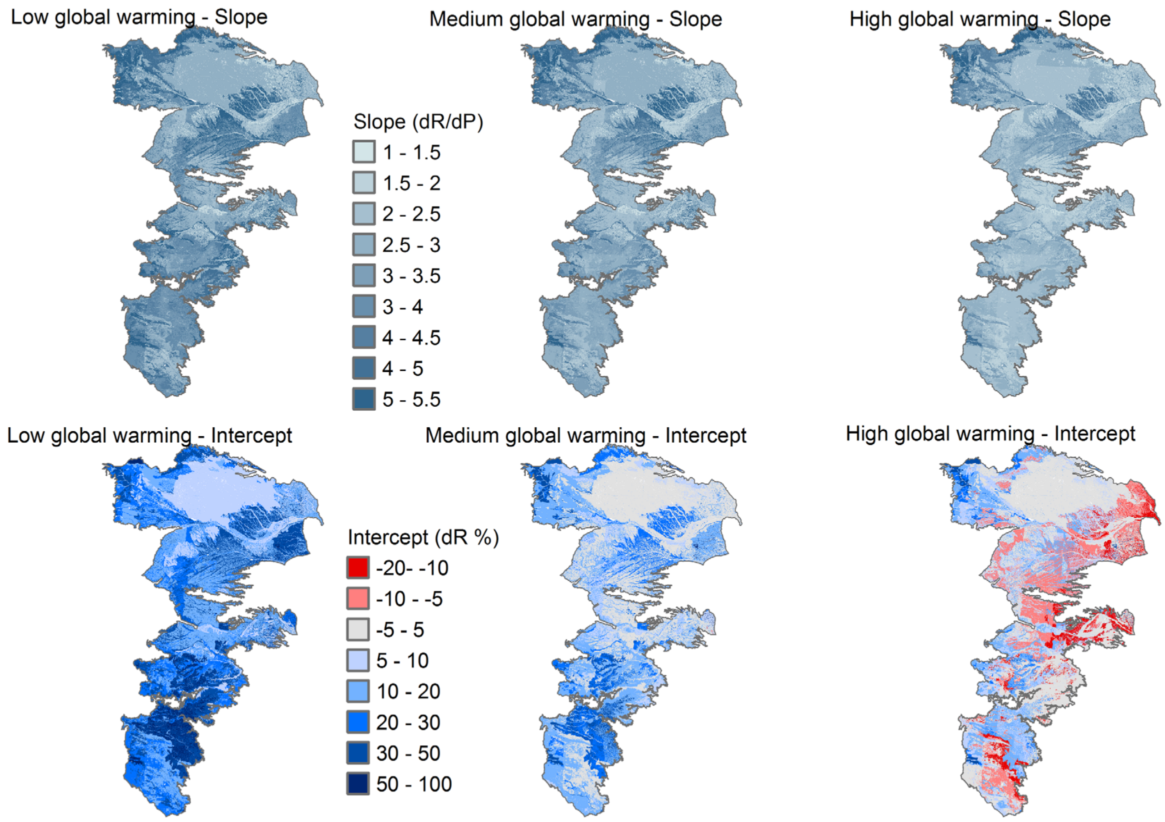

Figure 8. The slope and intercept of the relationship between a change in rainfall (d*P*) and a change in recharge (d*R*) at a grid cell scale for the entire High Plains. The slope is the sensitivity of recharge to a change in total rainfall and the intercept is the sensitivity of recharge to all other variables excluding the total change in rainfall.

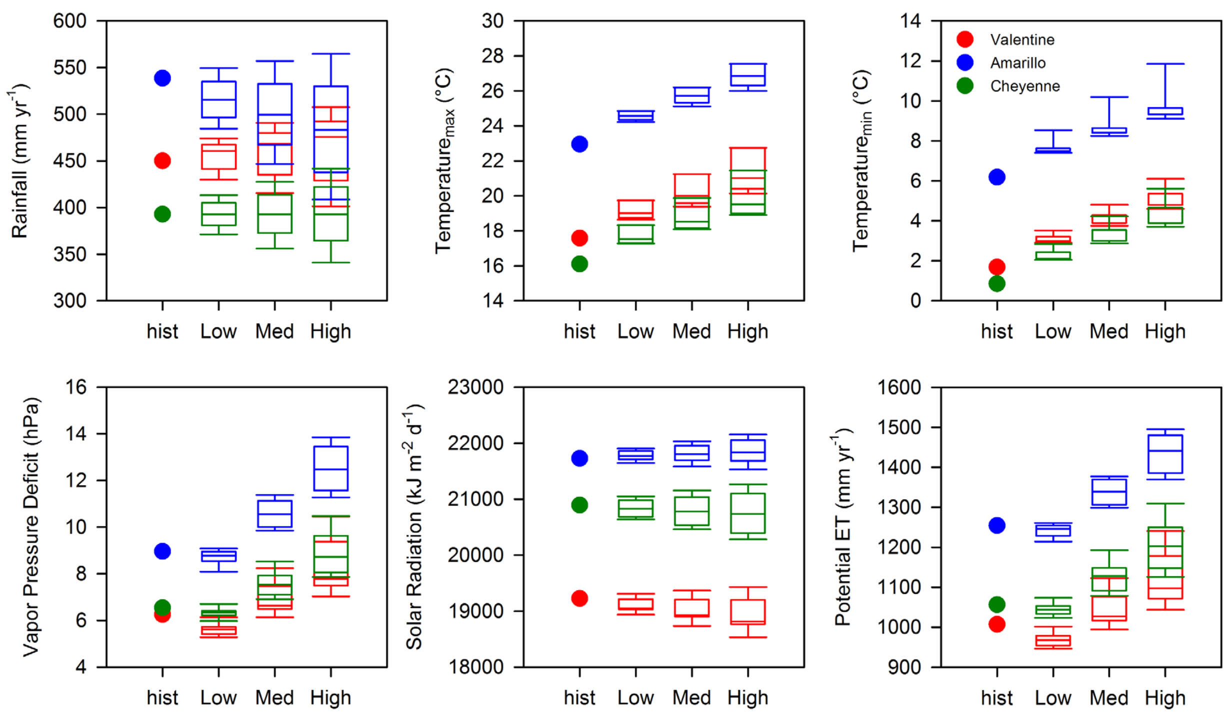

Figure 9. Mean annual climate variables for three climate stations. The historical (hist) mean is represented by a circle and the 16 GCM projections are represented by boxplots for each global warming scenario (low, medium, and high).

[51] Changes in PET across all three sites show the same trend as VPD, a decrease for the low global warming scenario and then an increase with further increases in global warming (Figure 9). Although the radiation and temperature both appear in equation (3), it is the changes in VPD that dominate the changes in PET and consequently affect recharge. Although annual PET changes may not be expected to affect recharge because annual PET is much greater than precipitation, it may have significant influence on daily scales by reducing the number or extent to which rainfall events temporarily exceed PET.

[52] One previous study from Uganda [*Kingston and Taylor*, 2010] showed increases in recharge (baseflow) with low levels of global warming and then decreases with higher global warming. The mechanism described for the initial increases in recharge with low global warming and then decreases with further global warming in Uganda differ from that shown in this study in that seasonality of projected rainfall in Uganda changed from a historical bimodal system to a unimodal system.

5.2. Comparison With Previous Studies in the High Plains

[53] Two previous studies investigated recharge under a future climate in the High Plains. *Rosenberg et al*. [1999] used three GCMs in the NHP and CHP and for all scenarios considered, a reduction in recharge was projected (up to −55% in the NHP and −77% in the CHP). This is considerably different to the results shown here, where the range of projections for the NHP and CHP cover both increases and decreases in recharge with a median case of a small increase in recharge for the NHP and an even smaller decrease in the CHP. This difference in results can be mainly attributed to the choice of GCMs used in each study. GISS is the only common GCM used between the *Rosenberg et al*. [1999] and the current study, but the data used are several generations apart. Figure 5 shows that it is possible to select three of the GCMs used in this study and obtain the result where all scenarios project a decrease in recharge. Another possible cause of the difference in results is due to model structure. Soil Water Assessment Tool (SWAT) [*Arnold et al*., 1998] and WAVES are very different models, but that has yet to be shown to be significant in projecting climate change effects on recharge [*Crosbie et al*., 2011].

[54] The other study was conducted at a point scale in the SHP using five GCMs chosen to cover the range of CMIP3 projections [*Ng et al*., 2010]. That study was consistent with this study in projecting future recharge (for 2090) in a range that encompasses both increases and decreases in recharge with a range of −75% to +35% compared to the results shown here (for 2050) for the SHP as a whole of −50% to +25%. The *Ng et al*. [2010] study would be expected to produce more extreme results than the current study as it is projecting further into the future, and the summary results from this study are based on 10 and 90% exceedances and not the full range of results.

[55] The advantages of the present study are that we have made projections for the entire High Plains Aquifer in a consistent way at a spatial resolution that allows local scale differences to be evaluated and therefore used by water managers.

5.3. Implications for Water Resources Management

[56] The highly uncertain projections for future recharge in both direction and magnitude of change mean that making specific recommendations for groundwater management is difficult. For the areas in the CHP and SHP where the current groundwater management is focused on planned depletion of storage, then the impact of changes in recharge upon water resources management will be minimal. Although the median projection for these areas is for a reduction in recharge, due to the thick unsaturated zone, these changes may not affect the water table for decades or centuries [*McMahon et al*., 2006]. In the NHP, where the management goal is maintaining base flow, the median projection for a small increase in recharge would provide an increase in the availability of water that could aid in maintaining groundwater levels at their present elevation.

[57] Due to the uncertain nature of future groundwater recharge rates under climate change, water resource management decisions based on deterministic projections are not recommended. Rather, probabilistic projections using the probability distributions fitted to the RSF rasters for given values of RSF allow the likelihood of changes with potential management consequences to be assessed [*Crosbie et al*., 2013]. For example, in areas where groundwater extractions are limited by water inputs then a 20% decrease (RSF = 0.8) in recharge could lead to a reduction in water allocations, and conversely, a 20% increase (RSF = 1.2) in recharge could lead to an increase in water allocations. The probability of exceeding a RSF of 0.5, 0.8, 1.0, and 1.2 has been evaluated for the high global warming scenario (Figure 10) and the average results reported for each region and state (Table 6).

[58] For most of the High Plains, there is greater than a 90% probability of exceeding a RSF of 0.5 (half the historical baseline), it is only Texas and New Mexico that have a greater than 10% probability of not exceeding a RSF of 0.5 (Table 6). For a RSF of 0.8, there is an 80% probability of exceedance for the NHP but less than a 50% probability of exceedance for the SHP. The probability of exceeding a RSF of 1.0 is the probability of an increase in recharge under a future climate; it is only the three northern most states (SD, WY, and NE) that have a probability of greater than 50% for an increase in recharge. None of the regions or states considered has a probability of greater than 50% of exceeding a RSF of 1.2.

6. Conclusions

[59] The aims of this study were threefold: (1) to produce projections of the change in recharge under a 2050 climate relative to 1990 climate, (2) to investigate whether the sensitivity of recharge to climate change differs under different vegetation types, and (3) to provide the findings in a way that is useful for water resources management. Each of these objectives has been met through consideration of 48 different projections of future recharge derived from climate projections produced by the 16 GCMs and three global warming scenarios. These scenarios provided atmospheric boundary conditions for point-scale numerical modeling in WAVES, the results of which were upscaled to the

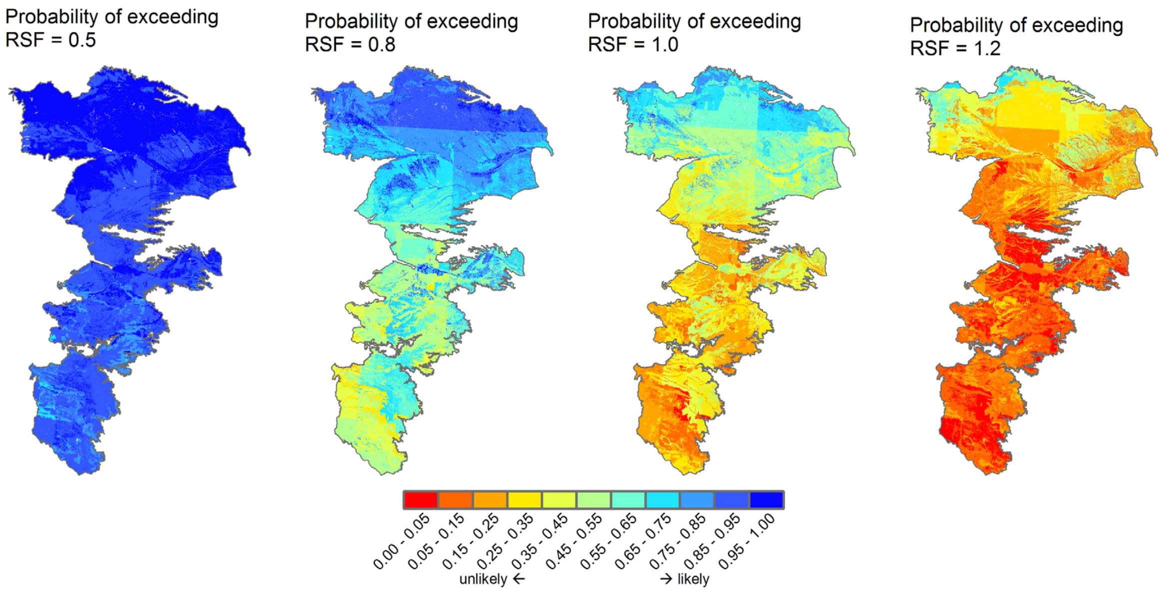

Figure 10. Probability of exceeding a given RSF under the high global warming scenario. (The low and medium global warming scenarios are shown in supporting information Figure S10).

entire aquifer. These have been simplified to three scenarios to enable the results to be communicated to water resource managers in a meaningful way.

[60] (1) For the NHP, the median projection is for a recharge scaling factor (RSF) of 1.08 (an 8% increase in recharge) with a range between the dry and wet scenarios of 0.76 and 1.32, respectively.

[61] (2) For the CHP, the median projection is for a RSF of 0.97 with a range between the dry and wet scenarios of 0.63 and 1.23, respectively.

[62] (3) For the SHP, the median projection is for a RSF of 0.90 with a range between the dry and wet scenarios of 0.50 and 1.25, respectively.

[63] Results show that vegetation is not necessarily a strong determinant of the sensitivity of recharge to climate change as sensitivity differs based on the amount of historical baseline recharge and not necessarily vegetation type (although vegetation type is a strong determinant of historical baseline recharge). Sensitivity of recharge to changes in rainfall is least for high baseline recharge and greatest for low baseline recharge. Sensitivity is greater than one, meaning that there is an amplification with greater changes in recharge than changes in rainfall. A surprising result was that in this water-limited environment (PET>>P), the change in recharge under a future climate is also quite sensitive to a change in PET. There is a general decrease in PET for the low global warming scenario that led to increases in recharge in many cases and then with further increases in global warming PET increased and caused a reduction in recharge.

[64] Overall, the projections of future recharge for the High Plains encompass both increases and decreases in recharge, meaning that management responses will need to be flexible enough to account for the uncertainty in recharge projections.

Table 6. Probability (p) of Exceeding a Given RSF for the High Global Warming Scenario for the NHP, CHP, and SHP Regions and Eight States of the High Plains

Region/State	p (RSF > 0.5)	p (RSF > 0.8)	p (RSF > 1.0)	p (RSF > 1.2)
NHP	0.96	0.80	0.55	0.28
CHP	0.91	0.57	0.28	0.10
SHP	0.88	0.49	0.24	0.09
South Dakota	0.97	0.87	0.71	0.48
Wyoming	0.97	0.83	0.66	0.44
Nebraska	0.97	0.82	0.58	0.28
Colorado	0.94	0.66	0.37	0.14
Kansas	0.93	0.63	0.32	0.12
Oklahoma	0.90	0.56	0.29	0.12
Texas	0.89	0.52	0.26	0.10
New Mexico	0.86	0.43	0.20	0.08

[65] **Acknowledgments.** We acknowledge the modeling groups, the Program for Climate Model Diagnosis and Intercomparison (PCMDI), and the WCRP's Working Group on Coupled Modeling (WGCM) for their roles in making available the WCRP CMIP3 multimodel data set. Support of this data set is provided by the Office of Science, U.S. Department of Energy. NCEP Reanalysis data provided by the NOAA/OAR/ESRL PSD, Boulder, Colorado, USA, from their Web site at http://www.esrl.noaa.gov/psd/. We would also like to acknowledge the insightful comments from the reviewers that greatly improved the quality of the paper.

References

Allen, R. G., L. S. Pereira, D. Raes, and M. Smith (1998), *Crop Evapotranspiration—Guidelines for Computing Crop Water Requirements*, Food and Agriculture Organization of the United Nations (FAO), Rome.

Arnold, J. G., R. Srinivasan, R. S. Muttiah, and J. R. Williams (1998), Large area hydrologic modelling and assessment. Part 1: Model development, *JAWRA J. Am. Water Resour. Assoc.*, *34*(1), 73–89, doi:10.1111/j.1752-1688.1998.tb05961.x.

Broadbridge, P., and I. White (1998), Constant rate rainfall infiltration: A versatile non-linear model: I. Analytical solution, *Water Resour. Res.*, *24*, 145–154.

Chiew, F. H. S., J. Teng, J. Vaze, D. A. Post, J. M. Perraud, D. G. C. Kirono, and N. R. Viney (2009), Estimating climate change impact on runoff across southeast Australia: Method, results, and implications of the modeling method, *Water Resour. Res.*, *45*, W10414, doi:10.1029/2008WR007338.

Colaizzi, P. D., P. H. Gowda, T. H. Marek, and D. O. Porter (2009), Irrigation in the Texas High Plains: A brief history and potential reductions in demand, *Irrig. Drain.*, *58*(3), 257–274, doi:10.1002/ird.418.

Cook, P. G., I. D. Jolly, G. R. Walker, and N. I. Robinson (2002), From drainage to recharge to discharge: Some timelags in subsurface hydrology, paper presented at Dubai International Conference on Water Resources and Integrated Management in the Third Millenium, Dubai, UAE, Feb. 2002.

Crosbie, R. S., B. Wilson, J. D. Hughes, C. McCulloch, and W. M. King (2008), A comparison of the water use of tree belts and pasture in recharge and discharge zones in a saline catchment in the Central West of NSW, Australia, *Agric. Water Manage.*, *95*(3), 211–223, doi:10.1016/j.agwat.2007.10.015.

Crosbie, R. S., I. D. Jolly, F. W. Leaney, and C. Petheram (2010a), Can the dataset of field based recharge estimates in Australia be used to predict recharge in data-poor areas?, *Hydrol. Earth Syst. Sci.*, *14*(10), 2023–2038.

Crosbie, R. S., J. L. McCallum, G. R. Walker, and F. H. S. Chiew (2010b), Modelling the climate change impact on groundwater recharge in the Murray-Darling Basin, *Hydrogeol. J.*, *18*(7), 1639–1656, doi:10.1007/s10040-010-0625-x.

Crosbie, R. S., W. R. Dawes, S. P. Charles, F. S. Mpelasoka, S. Aryal, O. Barron, and G. K. Summerell (2011), Differences in future recharge estimates due to GCMs, downscaling methods and hydrological models, *Geophys. Res. Lett.*, *38*, L11406, doi:10.1029/2011GL047657.

Crosbie, R. S., J. L. McCallum, G. R. Walker, and F. H. S. Chiew (2012), Episodic recharge and climate change in the Murray-Darling Basin, Australia, *Hydrogeol. J.*, *20*(2), 245–261, doi:10.1007/s10040-011-0804-4.

Crosbie, R. S., T. Pickett, F. S. Mpelasoka, G. Hodgson, S. P. Charles, and O. V. Barron (2013), An assessment of the climate change impacts on groundwater recharge at a continental scale using a probabilistic approach with an ensemble of GCMs, *Clim. Change*, *117*(1-2), 41–53, doi:10.1007/s10584-012-0558-6.

Dawes, W., L. Zhang, and P. Dyce (2004), *WAVES v3.5 User Manual*, 30 pp., CSIRO Land and Water, Canberra.

Green, T. R., B. C. Bates, S. P. Charles, and P. M. Fleming (2007), Physically based simulation of potential effects of carbon dioxide-altered climates on groundwater recharge, *Vadose Zone J.*, *6*(3), 597–609.

Green, T. R., M. Taniguchi, H. Kooi, J. J. Gurdak, D. M. Allen, K. M. Hiscock, H. Treidel, and A. Aureli (2011), Beneath the surface of global change: Impacts of climate change on groundwater, *J. Hydrol.*, *405*(3-4), 532–560.

Gurdak, J., and C. Roe (2010), Review: Recharge rates and chemistry beneath playas of the High Plains aquifer, USA, *Hydrogeol. J.*, *18*(8), 1747–1772, doi:10.1007/s10040-010-0672-3.

Holman, I., D. Allen, M. Cuthbert, and P. Goderniaux (2012), Towards best practice for assessing the impacts of climate change on groundwater, *Hydrogeol. J.*, *20*(1), 1–4, doi:10.1007/s10040-011-0805-3.

Holman, I. P., D. Tascone, and T. M. Hess (2009), A comparison of stochastic and deterministic downscaling methods for modelling potential groundwater recharge under climate change in East Anglia, UK: Implications for groundwater resource management, *Hydrogeol. J.*, *17*(7), 1629–1641.

Homer, C., J. Dewitz, J. Fry, M. Coan, N. Hossain, C. Larson, N. Herold, A. McKerrow, J. N. Van Driel, and J. Wickham (2007), Completion of the 2001 National Land Cover Database for the conterminous United States, *Photogramm. Eng. Remote Sens.*, *73*(4), 337–341.

Intergovernmental Panel on Climate Change (IPCC) (2007), *Climate Change 2007: The Physical Science Basis. Contribution of Working Group 1 to the Fourth Assessment Report of the Intergovernmental Panel on Climate Change*, 996 pp., Cambridge Univ. Press, Cambridge, U. K.

Kalnay, E., et al. (1996), The NCEP/NCAR 40-year reanalysis project, *Bull. Am. Meteorol. Soc.*, *77*(3), 437–471, doi:10.1175/1520-0477(1996)077<0437:tnyrp>2.0.co;2.

Kenny, J. F., N. L. Barber, S. S. Hutson, K. S. Linsey, J. K. Lovelace, and M. A. Maupin (2009), *Estimated Use of Water in the United States in 2005*, Circular 1344, 52 pp., US Geol. Surv., Reston, Va.

Kim, J. H., and R. B. Jackson (2012), A global analysis of groundwater recharge for vegetation, climate, and soils, *Vadose Zone J.*, *11*(1), doi:10.2136/vzj2011.0021RA.

Kingston, D. G., and R. G. Taylor (2010), Sources of uncertainty in climate change impacts on river discharge and groundwater in a headwater catchment of the Upper Nile Basin, Uganda, *Hydrol. Earth Syst. Sci.*, *14*(7), 1297–1308.

Luckey, R. R., and M. F. Becker (1999), Hydrogeology, water use, and simulation of flow in the High Plains aquifer in northwestern Oklahoma, southeastern Colorado, southwestern Kansas, northeastern New Mexico, and northwestern Texas, *Water-Resour. Invest. Rep. 99–4104*, 73 pp., U.S. Geol. Surv., Okla.

Luckey, R. R., D. A. Woodward, and C. P. Carney (2007), Simulated stream baseflow changes in the Nebraska Platte Basin above U.S. Highway 183 due to reduced groundwater irrigated land after July 1, 1997, 46 pp., Nebraska Dep. of Natural Resources, Cooperative Hydrology Study, Lincoln, Nebraska.

Maupin, M. A., and N. L. Barber (2005), *Estimated withdrawals from principal aquifers in the United States, 2000*, Circular 1279, 52 pp., U.S. Geol. Surv., Reston, Va.

McCallum, J. L., R. S. Crosbie, G. R. Walker, and W. R. Dawes (2010), Impacts of climate change on groundwater: A sensitivity analysis of recharge, *Hydrogeol. J.*, *18*(7), 1625–1638, doi:10.1007/s10040-010-0624-y.

McGuire, V. L. (2009), Water-level changes in the High Plains aquifer, predevelopment to 2007, 2005–06, and 2006–07, *U.S. Geol. Surv., Scientif. Invest. Rep. 2009–5019*, Reston, Va.

McMahon, P. B., K. F. Dennehy, R. L. Michel, M. A. Sophocleous, K. M. Ellett, and D. B. Hurlbut (2003), Water movement through thick unsaturated zones overlying the Central High Plains Aquifer, Southwestern Kansas, 2000–2001, *Water-Resour. Invest. Rep. 03–4171*, U.S. Geol. Surv., Reston, Va.

McMahon, P. B., K. F. Dennehy, B. W. Bruce, J. K. Böhlke, R. L. Michel, J. J. Gurdak, and D. B. Hurlbut (2006), Storage and transit time of chemicals in thick unsaturated zones under rangeland and irrigated cropland, High Plains, United States, *Water Resour. Res.*, *42*, W03413, doi:10.1029/2005WR004417.

Meehl, G. A., C. Covey, T. Delworth, M. Latif, B. McAvaney, J. F. B. Mitchell, R. J. Stouffer, and K. E. Taylor (2007), The WCRP CMIP3 multimodel dataset—A new era in climate change research, *Bull. Am. Meteorol. Soc.*, *88*(9), 1383–1394.

Mileham, L., R. G. Taylor, M. Todd, C. Tindimugaya, and J. Thompson (2009), The impact of climate change on groundwater recharge and runoff in a humid, equatorial catchment: Sensitivity of projections to rainfall intensity, *Hydrol. Sci. J.*, *54*(4), 727–738.

Monteith, J. L. (1965), Evaporation and environment, *The State and Movement of Water in Living Ogranisms*, *Symp. Soc. Exper. Biol.,* vol. *19*, Academic Press, N. Y.

Nakicenovic, N., and R. Swart (2000), *Special Report on Emission Scenarios*, 612 pp, Intergovernmental Panel on Climate Change, Cambridge University Press, Cambridge, U. K.

National Agricultural Statistics Services (2011), National Agricultural Statistics Services database. [Available at http://www.nass.usda.gov/index.asp.].

Ng, G. H. C., D. McLaughlin, D. Entekhabi, and B. R. Scanlon (2010), Probabilistic analysis of the effects of climate change on groundwater recharge, *Water Resour. Res.*, *46*, 7502–7502.

Natural Resources Conservation Service (NRCS) (2006), Natural Resources Conservation Service, United States Department of Agriculture. U.S. General Soil Map (STATSGO2). [Available at http://soildatamart.nrcs.usda.gov.].

Petheram, C., G. Walker, R. Grayson, T. Thierfelder, and L. Zhang (2002), Towards a framework for predicting impacts of land-use on recharge: 1. A review of recharge studies in Australia, *Aust. J. Soil Res*, *40*(3), 397–417.

Qi, S. L., A. Konduris, D. W. Litke, and J. Dupree (2002), *Classification of irrigated land using satellite imagery, the High Plains Aquifer, nominal date 1992*, 31 pp., U.S. Geol. Surv. Denver, Colo.

Rosenberg, N. J., D. J. Epstein, D. Wang, L. Vail, R. Srinivasan, and J. G. Arnold (1999), Possible impacts of global warming on the hydrology of the Ogallala Aquifer region, *Clim. Change*, *42*(4), 677–692.

Scanlon, B. R., and R. S. Goldsmith (1997), Field study of spatial variability in unsaturated flow beneath and adjacent to playas, *Water Resour. Res.*, *33*(10), 2239–2252, doi:10.1029/97wr01332.

Scanlon, B. R., M. Christman, R. C. Reedy, I. Porro, J. Simunek, and G. N. Flerchinger (2002), Intercode comparisons for simulating water balance of surficial sediments in semiarid regions, *Water Resour. Res.*, *38*(12), 1323–1323.

Scanlon, B. R., R. C. Reedy, D. A. Stonestrom, D. E. Prudic, and K. F. Dennehy (2005), Impact of land use and land cover change on groundwater recharge and quality in the southwestern US, *Global Change Biol.*, *11*(10), 1577–1593, doi:10.1111/j.1365–2486.2005.01026.x.

Scanlon, B. R., K. E. Keese, A. L. Flint, L. E. Flint, C. B. Gaye, W. M. Edmunds, and I. Simmers (2006), Global synthesis of groundwater recharge in semiarid and arid regions, *Hydrol. Process.*, *20*(15), 3335–3370.

Scanlon, B. R., R. C. Reedy, and J. A. Tachovsky (2007), Semiarid unsaturated zone chloride profiles: Archives of past land use change impacts on water resources in the southern High Plains, United States, *Water Resour. Res.*, *43*, W06423, doi:10.1029/2006WR005769.

Scanlon, B. R., R. C. Reedy, and J. B. Gates (2010a), Effects of irrigated agroecosystems: 1. Quantity of soil water and groundwater in the southern High Plains, Texas, *Water Resour. Res.*, *46*, W09537, doi:10.1029/2009WR008427.

Scanlon, B. R., R. C. Reedy, J. B. Gates, and P. H. Gowda (2010b), Impact of agroecosystems on groundwater resources in the Central High Plains, USA, *Agric. Ecosyst. Environ.*, *139*(4), 700–713.

Scanlon, B. R., C. C. Faunt, L. Longuevergne, R. C. Reedy, W. M. Alley, V. L. McGuire, and P. B. McMahon (2012), Groundwater depletion and sustainability of irrigation in the US High Plains and Central Valley, *Proc. Natl. Acad. Sci. U.S. A.*, *109*(24), 9320–9325, doi:10.1073/pnas.1200311109.

Sophocleous, M. (2004), Ground-water recharge and water budgets of the Kansas High Plains and related aquifers, *Geol. Surv. Bull. 249*, 102 pp., Kansas Geol. Surv.

Sophocleous, M. (2012), The evolution of groundwater management paradigms in Kansas and possible new steps towards water sustainability, *J. Hydrol.*, *414-415*, 550–559.

Szilagyi, J., V. A. Zlotnik, J. B. Gates, and J. Jozsa (2011), Mapping mean annual groundwater recharge in the Nebraska Sand Hills, USA, *Hydrogeol. J.*, *19*(8), 1503–1513, doi:10.1007/s10040-011-0769-3.

Taylor, R. G., et al. (2013), Ground water and climate change, *Nature Clim. Change*, *3*(4), 322–329, doi:10.1038/nclimate1744.

Wada, Y., L. P. H. van Beek, C. M. van Kempen, J. W. T. M. Reckman, S. Vasak, and M. F. P. Bierkens (2010), Global depletion of groundwater resources, *Geophys. Res. Lett.*, *37*, L20402, doi:10.1029/2010GL044571.

Wang, H. X., L. Zhang, W. R. Dawes, and C. M. Liu (2001), Improving water use efficiency of irrigated crops in the North China Plain—Measurements and modelling, *Agric. Water Manage.*, *48*(2), 151–167.

Weeks, J. B., E. D. Gutentag, F. J. Heimes, and R. R. Luckey (1988), Summary of the High Plains regional aquifer-system analysis in parts of Colorado, Kansas, Nebraska, New Mexico, Oklahoma, South Dakota, Texas, and Wyoming, *USGS Prof. Pap. 1400-A*, 39 pp., U.S. Geol. Surv., Denver, Colo.

Wohling, D. L., F. W. Leaney, and R. S. Crosbie (2012), Deep drainage estimates using multiple linear regression with percent clay content and rainfall, *Hydrol. Earth Syst. Sci.*, *16*(2), 563–572, doi:10.5194/hess-16–563-2012.

Wood, W. W., and W. E. Sanford (1995), Chemical and isotopic methods for quantifying ground-water recharge in a regional, semiarid environment, *Ground Water*, *33*(3), 458–468.

Wu, H., E. J. Rykiel, T. Hatton, and J. Walker (1994), An integrated rate methodology (IRM) for multi-factor growth rate modelling, *Ecol. Modell.*, *73*(1-2), 97–116.

Zhang, L., and W. Dawes (1998), *WAVES—An Integrated Energy and Water Balance Model*, 218 pp, CSIRO Land and Water, Canberra.

Zhang, L., W. R. Dawes, and T. J. Hatton (1996), Modelling hydrologic processes using a biophysically based model—Application of WAVES to FIFE and HAPEX-MOBILHY, *J. Hydrol.*, *185*(1-4), 147–169.

Zhang, L., W. R. Dawes, T. J. Hatton, I. H. Hume, M. G. O'Connell, D. C. Mitchell, P. L. Milthorp, and M. Yee (1999), Estimating episodic recharge under different crop/pasture rotations in the Mallee region. Part 2. Recharge control by agronomic practices, *Agric. Water Manage.*, *42*(2), 237–249.